Synthesis and Thermal Degradation Kinetics of Poly(methacrylamide)/Clay Nanocomposites using Intercalated Monomer Method

Monomer Arakatkısı Yöntemi İle Poli(metakrilamid)/Kil Nanokompozitlerinin Sentezi ve Isıl Bozunma Kinetiği

Research Article

Esra Evrim Yalçınkaya
Ege University, Faculty of Science, Chemistry Department, Bornova/Izmir, Turkey.

ABSTRACT

A novel method was used successfully for the synthesis of poly(methacrylamide)-montmorillonite (PMAA/Mont) nanocomposites. Methacrylamide (MAA) was first intercalated into the interlayer regions of clay minerals by ion exchange reaction. The intercalation of monomers into Mont was confirmed by FTIR, XRD and TGA techniques. Then, the monomers polymerized within the montmorillonite (Mont) layers for preparation of nanocomposites in different clay loading degrees. The morphology and thermal behaviors of nanocomposites were found to be strongly dependent on the clay content. XRD and SEM analysis indicated that the resultant nanocomposites exhibited intercalated morphologies with homogeneous clay platelet distribution. The Kissinger method was used for the calculation of the decomposition activation energy. Activation energies of PMAA/Mont nanocomposites are higher than those of neat PMAA, indicating that addition of clay mineral improves thermal stability of neat polymer.

Key Words
Nanocomposites, Poly(methacrylamide), clay, thermal degradation, Kissinger method.

ÖZ

Poli(metakrilamid)-montmorillonit (PMAA/Mont) nanokompozitlerinin sentezi için yeni bir yöntem başarıyla bu çalışmada uygulanmıştır. Öncelikle metakrilamid (MAA) monomeri, kil mineralinin tabakaları arasına iyon değişim tepkimesi ile yerleştirilmiştir. Montmorillonitin ara tabakalarına yerleştirilen monomer FTIR, XRD ve TGA yöntemleri ile karakterize edilmiştir. Daha sonra, farklı yüzdelerde kil içeren nanokompozitlerin hazırlanması amacıyla monomer montmorillonitin tabakaları arasında polimerleştirilmiştir. Nanokompozitlerin morfolojik ve ısıl özelliklerinin büyük oranda kil miktarına bağlı olduğu saptanmıştır. XRD ve SEM analizleri, nanokompozitlerin kil tabakalarının homojen dağılmasıyla oluşan intercalated morfolojisine sahip olduğunu göstermiştir. Bozunma aktivasyon enerjisinin hesaplanması amacıyla Kissinger yöntemi kullanılmıştır. PMAA/Mont nanokompozitlerinin aktivasyon enerjilerinin katkısız PMAA'nın aktivasyon enerjisinden daha büyük olduğu görülmüştür. Bu sonuç, kil mineralinin eklenmesi ile katkısız polimerin ısıl kararlılığının arttığını göstermektedir.

Anahtar Kelimeler
Nanokompozitler, Poli(Metakrilamid), kil, ısıl bozunma, Kissinger yöntemi.

Article History: Received: May 24, 2016; Revised: Sep 7, 2016; Accepted: Oct 20, 2016; Available Online: Dec 31, 2016.

DOI: 10.15671/HJBC.2016.118

Correspondence to: E.E. Yalçınkaya, Ege University, Faculty of Science, Chemistry Department, Bornova/Izmir, Turkey.
Tel: +90 232 311 1778 Fax: +90 232 388 8264 E-Mail: esra.evrim.saka@ege.edu.tr

INTRODUCTION

The field of nanotechnology is one of the most popular areas for current research and development in basically all technical disciplines. This obviously includes polymer science and technology and even in this field the investigations cover a broad range of topics. Even in the field of nanocomposites, many diverse topics exist including composite reinforcement, barrier properties, flame resistance, thermal properties, dielectric properties, cosmetic applications, bactericidal properties [1-5].

In general, polymer nanocomposites are obtained by the dispersion of inorganic or organic nanoparticles into polymer matrix. The key to the successful development of clay based nanocomposites is to achieve exfoliation of the layered silicate in the polymer matrix. The three most common methods to synthesize polymer based nanocomposites are intercalation of polymer from solution, polymer melt intercalation and in situ polymerization. In intercalative polymerization method, the monomer, together with the initiator and catalyst, is intercalated within the silicate layers and the polymerization is initiated either thermally or chemically in situ [6-8]. The chain growth in the clay galleries triggers the clay exfoliation and, hence, the nanocomposite formation. Among them, dispersing in situ polymerization may be the most desirable method for preparing nanocomposites because the types of nanoparticles and the nature of polymer precursors can vary in a wide range to meet the requirements.

Methacrylamide (MAA) has been widely applied on industrial scale. It is one of the most important vinyl monomer for large polymer-add-on can be easily obtained because of the hydrophilic nature of the MAA [9]. Polymers based on methacrylamide with very high molecular weights have gained more and more technical attention due to the solubility into water. It is relatively less toxic, polar and less expensive than other vinyl monomers. However, poor thermal and mechanical properties especially thermal stability need to be improved. Different inorganic nanoparticles could be used to prepare of PMAA nanocomposites such as laponite [10], hectorite [11], kaolinite [12], graphite[13], Z,n0.4Ni0.5Cu0.1Fe_2O_4 particles [14] due to improve these properties.

Different polymers and methods were used for synthesis of the nanocomposites in our previous works. For example, Yalçınkaya et al. prepared polynorbornadiene/clay nanocomposiyes with intercalated catalysis methods. The thermal and dielectric properties were also investigated [4]. In other work, polyvinylimidazole/MMT nanocomposites were synthesised exhibiting good thermal stability and physical properties [5]. Also polynorbornene/clay nanocomposites were prepared in stu method and also the dielectric properties were investigated [15]. In this study, PMAA/Mont nanocomposites synthesized and characterized in detailed using in situ polymerization method, with intercalated MAA monomer into Mont layers. This method is the first example of in situ polymerization of MAA monomers within the Mont layers for preparation of nanocomposites in different clay loading degrees. The structures of nanocomposites were determined by X-ray Diffraction (XRD) and Scanning Electron Microscopy (SEM). Furthermore, the Kissinger method was used to estimate the thermal decomposition activation energy for PMAA/Mont nanocomposites.

MATERIALS and METHOD

Materials

Methacrylamide monomer was supplied from Sigma-Aldrich. The Na-MMT (cation exchange capacity=92 meq/100 g) was supplied by Southern Clay Products, Inc. Commercial grade solvents were also dried under Argon atmosphere and distilled prior to use. All other chemicals were reagent grade. Potassium persulfate (Sigma-Aldrich) was used as an initiator. Ascorbic acid (Merck) was used as a reducing agent.

Preparation of Intercalated Monomer (MAA/Mont)

The intercalated Mont was prepared by the method of ion exchange reaction. The amount of MAA was equivalent to 2.0 times cation exchange capacity (CEC) of Mont. The intercalating agent was firstly protonated with 1.0 M HCl aqueous

solutions to adjust the pH to 2.0–3.0. An aqua solution was prepared by dissolving 0.02 mol of MAA in 40 mL distilled water and heated to 50°C. Na-Mont powder (0.5 g) was dispersed in 200 mL deionized water under stirring for about 24 h to obtain well dispersed. Then, it was slowly dropped into the Mont dispersion for stirring 24 h at 50°C. The modified clay (designed as MAA/Mont) was separated by filtration and washed several times with deionized water until no chloride ions were detected by $AgNO_3$ solution. The MAA/Mont samples was dried in a vacuum oven for 2 days.

Preparation of the PMAA/Mont Nanocomposites by In situ Intercalative radical polymerization

PMAA was synthesized by a solution polymerization method. MAA/Mont (1, 2, and 3% of the monomer by weight) were placed to shelenk under Argon atmosphere and dispersed in distilled water. 9.7 mmol (1 mL) MAA was pipetted into the shelenk with freshly prepared solutions of 0.05 M (2 mL) Potassium persulfate and 0.05M (2 mL) Ascorbic acid. The reaction was stirred at room temperature for 30 min and placed in an oil bath at 65°C for 24h. The nanocomposites were precipitated in the excess amount of acetone, redissolved in methanol, and precipitated a second time into acetone. The yields were separated with ultracentrifugation followed washing with acetone several times. It was dried in a vacuum oven for overnight.

Characterization

Characterization of the interlayer spacing of the Na-Mont, MAA/Mont and nanocomposites were determined by means of X-Ray Diffraction Spectrometer (Philips E'xpert Pro; Cu-K ray, =1.54056 Å). Also, description type of the nanocomposites was defined by this method. The basal spacing values of Mont were calculated by Bragg's Law ($n\lambda=2d\sin\theta$). FTIR spectra were obtained by using Perkin Elmer Spectrum 100 FTIR Spectrometer. Thermogravimetric analysis (TGA) were performed on Perkin Elmer Pyris 1 TGA/DTA by heating the samples from ambient temperature to 600°C at 10°C/min. Also, for the thermal kinetic analysis, samples were heated at heating rates of 5, 10, 15 and 20°C per min from room temperature to 600°C under nitrogen atmosphere. Fracture surfaces of the nanocomposites were investigated by SEM analysis using Philips XL-30S FEG instrument.

RESULTS and DISCUSSION

For the preparation of the PMAA/Mont nanocomposites includes a two-step reaction that is schematically demonstrated as follows (Figure 1): at first, the pre-intercalation of pristine Mont fillers was performed in the presence of MAA monomer. For this purpose, the clay (Na-Mont) was dispersed in MAA by intensive mixing at room temperature for 24 h until the intercalation of MAA monomer between silicate interlayer species was achieved (Figure 1a). For the complete polymerization of MAA monomers between silicate galleries, interlamellar in situ polymerization of MAA was carried out by radical polymerization using different ratios of MAA preintercalated Mont (Figure 1b).

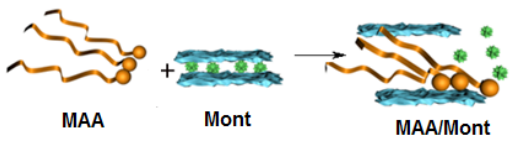

Figure 1a. The Cation-Exchange Process.

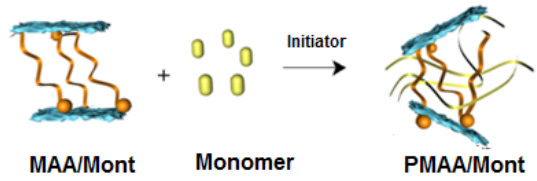

Figure 1b. The In-Situ Polymerization Process.

The intercalation of MAA monomer to clay mineral was characterized by FTIR and XRD. Thermal stability of pristine and modified Mont was also determined with TGA analysis. For the characterization, samples were first examined with a FTIR. For analysis, the samples were mixed with dry KBr, the pellets were prepared and processed further to obtain FTIR data which was transferred to the PC to acquire the spectra. As shown in the FTIR spectra (Figure 2), pristine Mont showed a typically broad O-H stretching band at 3630 cm^{-1}. The strong peak at 1620 cm^{-1} and the broad band at 3450 cm^{-1} have been assigned to the bending and stretching modes of adsorbed water. It showed a broadly similar pattern of absorption at the 1040 cm^{-1} arising

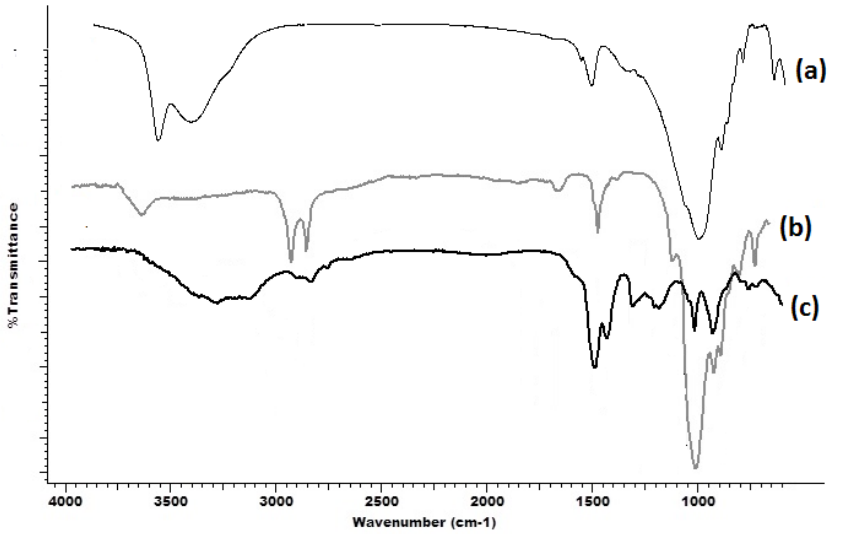

Figure 2. FTIR spectrum of (a) Mont, (b) MAA/Mont and (c) PMAA/1% Mont.

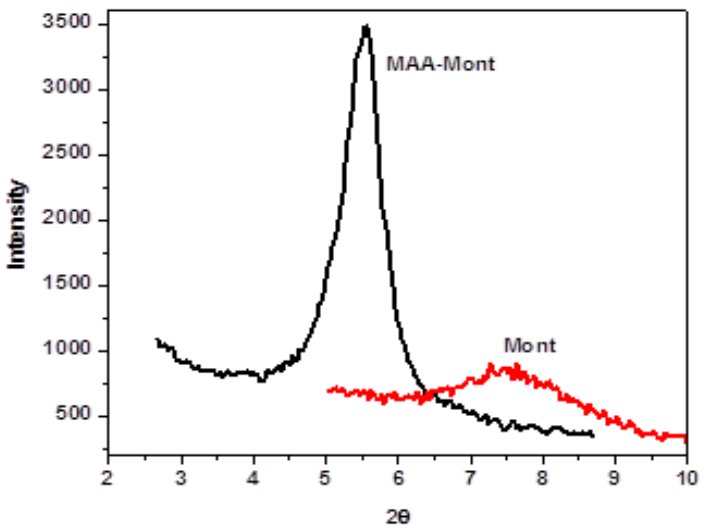

Figure 3. XRD pattern of Mont and MAA/Mont.

from Si-O stretching vibrations. In addition to Mont bands, the most important band of MAA/Mont was observed at around 2800-2900 cm^{-1} which is attributed to the presence of N-H and C-H stretching band in MAA. FTIR spectrum of PMAA/1% Mont nanocomposite (other results not shown in Figure) shows the peaks of both PMAA and Mont such as the characteristic Mont absorption bands (1050 cm^{-1}) and PMAA absorption bands (2900 cm^{-1}) (Figure 2c).

The intercalation of MAA to Mont was also confirmed by XRD. The basal spacing values of MAA/Mont were compared with pristine Mont to indicate the presence of MAA monomers. The diffractograms of these structures were presented in Figure 3. The typical XRD reflection of Na-Mont related to the basal spacing between the clay mineral platelets appeared at 2θ=7.657. The basal (interlayer) spacing value (d_{001}) of Mont was calculated from this value as 11.40 Å by using the Bragg's law: $d=n\lambda/(2\sin\theta)$. This reflection shifted to 2θ = 5.431° in the spectrum of MAA/Mont, and the corresponding interlayer spacing of MAA/Mont was calculated as d_{001} = 16.25 Å. This reflection appeared at the lower angles of the diffractogram indicated the intercalation of MAA monomers in the interlayer spaces of MAA/Mont.

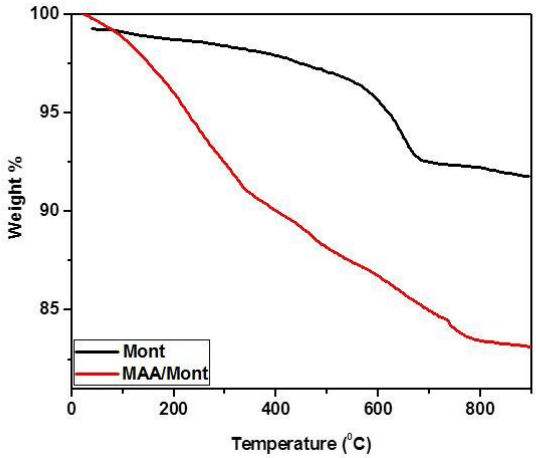

Figure 4. FTIR spectrum of (a) Mont, (b) MAA/Mont and (c) PMAA/1% Mont.

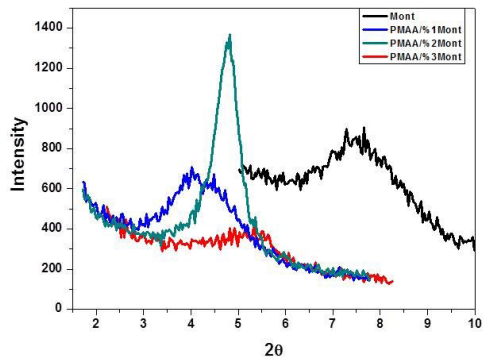

Figure 5. XRD pattern of neat Mont and different percentage PMAA/Mont nanocomposites.

The d-spacing value of organoclay mineral MAA/Mont increased from 11.40 Å to 16.25 Å for MAA substituent with the long chain structure. The increasing of basal spacing values of Mont could be seen clearly due to the increasing of interlayer distance of the Mont. It is evident that the MAA was entered the interlayer space of the Mont.

The thermal stability of Mont and MAA/Mont were investigated with TGA analysis. The TGA thermograms of Mont and MAA/Mont were shown in Figure 4. Mont exhibited about 9 wt % loss at 800°C due to the presence of volatile materials. Degradation started at 100°C because of the unbounded H_2O and continued up to about 800°C due to the chemically bound H_2O. The weight lost in MAA/Mont was found as 20 weight % due to the presence of MAA as a modifier. Hence, it was indicated that 11 weight % modifier was hold on to the Mont structure. The thermal stability of the modified clay mineral were found lower than that of unmodified clay mineral as reported in previous papers [16-17].

XRD patterns of the nanocomposites in the range of 2θ=1-10 revealed the basal spacing (d) between the silicate layers of organoclays. A left-shift in the peak indicates an increase in the d_{001} of the silicate layers, whereas the disappearance of a characteristic peak can be an indication of exfoliated structure or poor dispersion of the clay [18]. Figure 5 shows the XRD patterns of the nanocomposites as well as that of neat clay. The basal spacings of the neat clay was 11.40 Å. Peak shifts were more apparent for the nanocomposites prepared with monomer intercalated Mont. The basal spacings of the nanocomposites were calculated as 17.62, 16.61 and 16.27 Å for PMAA/1% Mont, PMAA/2% Mont and PMAA/3% Mont, respectively. Changes in

Table 1. XRD data for Mont and PMAA nanocomposites.

Clays and nanocomposites	d_{001} (Å)
Na-Mont	11.40
MAA/Mont	16.25
PMAA/1% Mont	17.62
PMAA/2% Mont	16.61
PMAA/3% Mont	16.27

the d-spacing values calculated from the XRD patterns were in accordance with the reports in the literature. For nanocomposites, the diffraction angle of the characteristic peaks was lower than that of MAA/Mont. However, none of the nanocomposites exhibited a clear disappearance of the basal reflection peak. The increase in basal spacing values can be attributed to the presence of exfoliated or intercalated structure, since in general, delamination of the silicate layers prevents X-ray diffraction from the layers resulting in the disappearance of the diffraction peaks [19]. The basal spacing (d_{001}) of the all materials were summarized in Table 1. Clearly, modified clay and nanocomposites always show larger d spacing when in comparison to that of unmodified clay.

Thermogravimetric analysis (TGA) is a useful technique to assess the degradation behavior and composition of composites [20,21]. The thermal stability of the PMAA matrix and PMAA nanocomposites were shown in Figure 6. The thermal degradation of PMAA took place in two major steps in the range of 210–250°C and 320–420°C. As indicated by the TGA, the thermal decomposition temperature increases slightly with increasing Mont percentage, indicating that the addition of Mont clay improves the thermal stability. Correspondingly, the residues of the Mont containing nanocomposites are larger than that of the PMAA and closely related to the clay contents in the PMAA. The PMAA/Mont nanocomposites have obviously greater char yield, which increases upon increasing the clay content, as expected.

The morphology and dispersion of the clay nanofibers in the polymeric matrices are investigated by SEM. As shown in the SEM photographs of the PMAA/Mont nanocomposites at magnification 5000x (Figure 7), there are many uniform light dots in the images of PMAA/Mont nanocomposites and the light dots are probably the fractured ends of the bundles of the rod-shaped PMAA. The all dispersion of Mont in the PMAA matrix is homogeneous due to chemical modification of the PMAA. During the intercalative polymerization process, the layer structure of the montmorillonite suffered tremendous damage and was exfoliated from expansion induced by the PMAA molecular size increasing and the exothermal reaction between the galleries [22,23]. Figure 7 shows that after polymerization, the montmorillonite aggregates are broken into small particles and dispersed homogeneously in the PMAA matrix. It was clearly observed that the nanocomposites surfaces exhibited a rough surface after this composition step. The clay platelets were stacked together in a disordered pattern to form agglomerates in some parts, and small and well-separated particles were also observed. For the PMAA/1% Mont, has relatively small clusters of the clay particles that are homogeneously dispersed in the PMAA matrix. On the other hand, the other nanocomposites big aggregated particles can be seen together with small aggregates. These changes in the morphologies indicate that the intercalation was accompanied.

Kinetic data obtained from TGA is very helpful to understand the thermal degradation processes and mechanisms, and also may be used as input parameters for a model of thermal degradation reaction [24]. PMAA/3% Mont nanocomposite was selected for the kinetic study of thermal degradation, due to its highest thermal stability. The neat PMAA and PMAA/3% Mont heated thermogravimetrically under

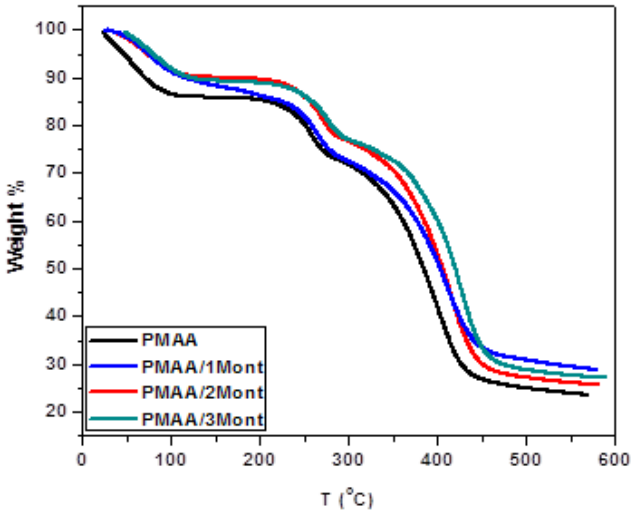

Figure 6. TGA of neat PMAA and PMAA/Mont nanocomposites.

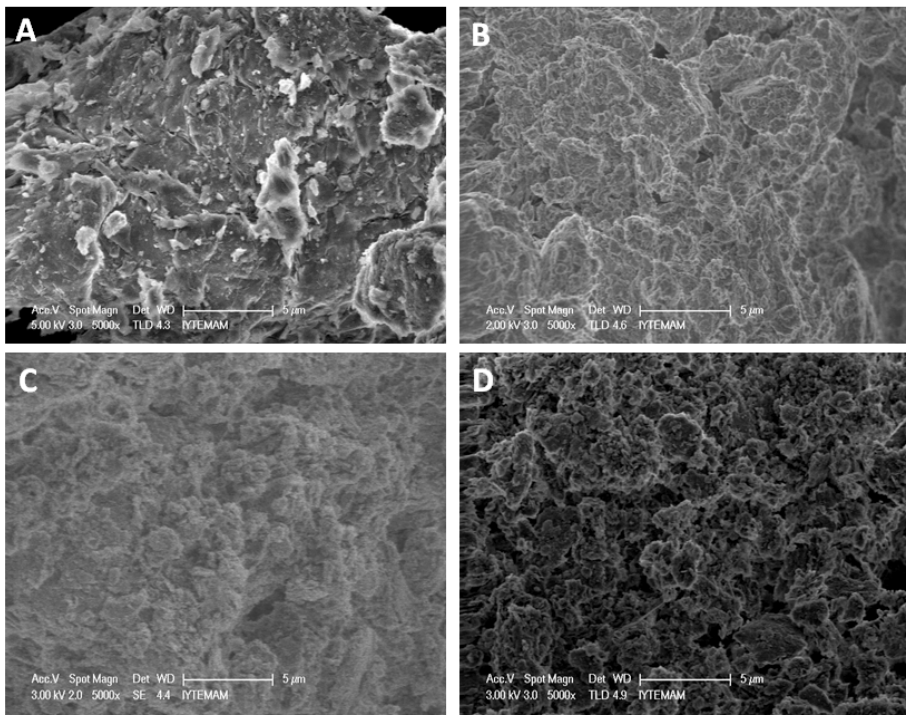

Figure 7. SEM micrograph of (A) neat Mont, (B) PMAA/1% Mont, (C) PMAA/2% Mont, (D) PMAA/3% Mont, with 5000x.

various heating rates such as 5, 10, 15, and 20°C min^{-1} in a temperature range of 25 to 600°C to determine their thermal degradation activation energies. The TG curves obtained for neat PMAA and PMAA/3% Mont are shown in Figures 8(a) and 8(b), respectively. The individual degradation behavior of each compound was analogous at all heating rates as seen from the figure. The activation energies for the compounds were estimated by the Kissenger method, without a precise knowledge of the reaction mechanism by using Equation (1) [25].

where, β is the heating rate; Tmax is temperature related to maximum reaction rate; A is the pre-exponential factor; Ea is the activation energy;

$$\ln\left(\frac{\beta}{T_{max}^{2}}\right) = -\frac{E_a}{RT_{max}} + \left\{\ln\frac{AR}{E_a} + \ln\left[n\left(1-\alpha_{max}\right)^{n-1}\right]\right\}$$

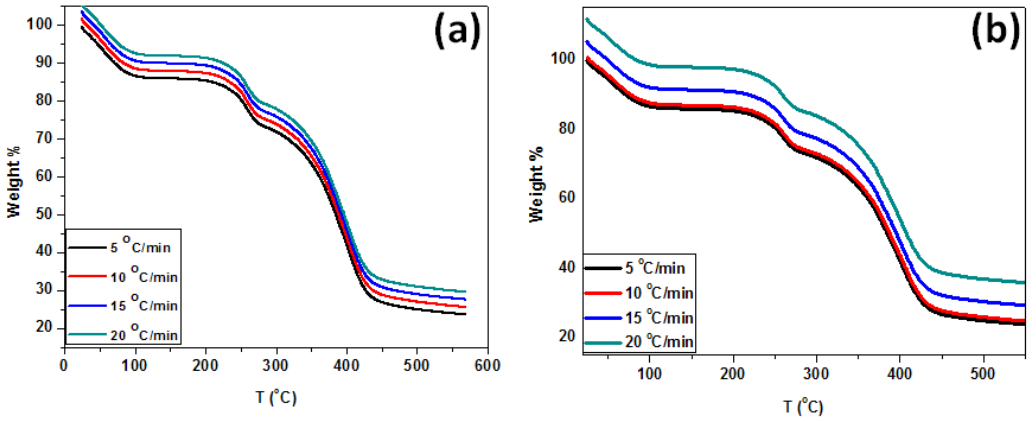

Figure 8. The TG thermograms of (a) neat PMAA and (b) PMAA/3% Mont in argon atmosphere at different heating rates. (5, 10, 15 and 20°C min^{-1})

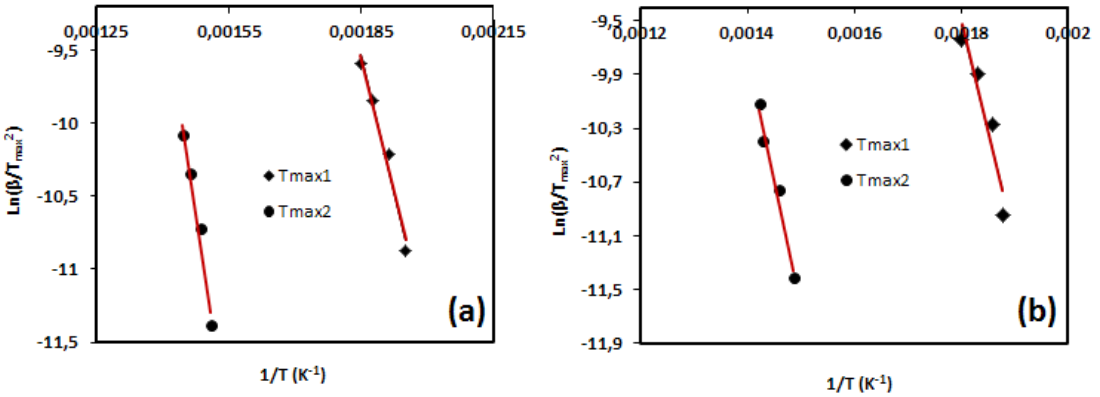

Figure 9. The plots used for the determination of the activation energies of (a) PMAA and (b) PMAA/3% Mont nanocomposite according to the Kissenger method.

α_{max} is the maximum conversion and n is the order of the reaction. From a plot of Ln(β/T_{max}^2) versus 1/Tmax, and fitting to a straight line, the activation energy E_a can be calculated from the slope (Figure 9a,b). The kinetic parameters for thermal degradation are calculated considering the heating rates of 5, 10, 15 and 20°C/min for first and second stages, and the results are summarized in Table 2. The results reveal that the activation energy at both stages for PMAA/3% Mont nanocomposite are higher when compared to those of neat PMAA. The activation energies determined by the Kissenger method indicate that the thermal stability of PMAA/3% Mont has a significantly higher ◦ value than that of neat PMAA. Thus, it is shown that the addition of the clays increases the thermal stability.

Conclusions

In this work, PMAA/Mont nanocomposites were successfully prepared by the in situ radical polymerization of intercalated methacrylamide monomers. The polymerization of methacrylamide monomer through the interlayer galleries leads to nanocomposites formations, which are formed by individually dispersing inorganic silica nanolayers in the polymer matrix. These nanocomposites showed a mixture of morphology, mainly intercalated morphology. The thermal properties of the nanocomposites demonstrated an improvement in the thermal stability compared to that of the neat polymer. An average improvement of 35°C was obtained for PMAA/3% Mont nanocomposites with 3% reinforcements when 50% of the materials were

Table 2. The activation energies of PMAA and PMAA/3% Mont Nanocomposite obtained by Kissinger Method.

samples at different stages	Slope	E_a (kJ/mol)	R^2
PMAA (first stage)	-12319	102	0.9795
PMAA (second stage)	-20043	166	0.9729
PMAA/3% Mont (first stage)	-16273	135	0.9557
PMAA/3% Mont (second stage)	-20704	173	0.9833

degraded. A comparison between the activation energies for the thermal degradation of PMAA and PMAA/Mont via the Kissinger method pointed out that there was a significant trend for the increase of the evident activation energy of the nanocomposite.

References

1. P. Kiliaris, C.D. Papaspyrides, Polymer/layered silicate (clay) nanocomposites: An overview of flame retardancy, Progress Polymer Science. 35 (2010) 902-958.
2. E.P. Giannelis, Polymer Layered Silicates Nanocomposites, Advances Materials. 8 (1996) 29-35.
3. T.J. Pinnavaia, G.W. Beall, Polymer-Clay Nanocomposites, Wiley, Chichester, UK. (2000)
4. E.E. Yalcinkaya, M. Balcan, C. Guler, Synthesis, characterization and dielectric properties of polynorbornadiene-clay nanocomposites by ROMP using intercalated Ruthenium catalyst, Material Chemistry and Physics. 143 (2013) 380-386.
5. M.Lan, P. D. Kaviratna, T. J. Pinnavaia, On the nature of polyimide–clay hybrid composites, Chemistry Materials, 6 (1994) 573-575.
6. S.S. Ray, M. Bousmina, Biodegradable polymers and their layered silicate nanocomposites: In greening the 21st century materials World, Progress Polymer Science, 50 (2005) 962-979.
7. Q.T. Nguyen, D.G. Baird, Preparation of polymer-clay nanocomposites and their properties, Advances Polymer Technology, 25 (2006) 270-285.
8. F. Hussaın, M. Hojjatı, M. Okamoto, R.E. Gorga, Polymer-matrix nanocomposites, processing, manufacturing, and application: an overview, Journal of Composites Materials, 40 (2006) 1511-1575.
9. Y. Kawahara, M. Shioya, Mechanical properties of tussah silk fibers treated with methacrylamide, Journal of Applied Polymer Sience, 65 (1997) 2051-2057.
10. Q. Zhang, X. Li, Y. Zhao, L. Chen, Preparation and performance of nanocomposite hydrogels based on different clay, Applied Clay Science, 46 (2009) 346-350.
11. R. Anbarasan, P. Arvind, V. Dhanalakshmi, Synthesis and characterization of Polymethacrylamide–Clay nanocomposites, Journal of Applied Polymer Sience, 121 (2011) 563-573.
12. T.A. Elbokl, J. Detellier, Kaolinite-poly(methacrylamide) intercalated nanocomposite via in situ polymerization, Canadıan Journal of Chemıstry-Revue Canadıenne De Chimie, 87 (2009) 272-279.
13. J.L. Liang, J. P. Bell, D. A. Scola, Preparation and characterization of electropolymerized poly(N-substituted methacrylamide) matrices on graphite fibers, Journal of Applied Polymer Sience, 48 (1993) 477–494.
14. H. Qui, F. Xu, L. Li, C. Xiang, Polyacrylamide/Zn 0.4 Ni 0.5 Cu 0.1 Fe 2 O 4 nanocomposites: synthesis, characterization and electromagnetic properties, Materials Chemistry and Physics, 124 (2010) 1039-1045.
15. E.E. Yalcinkaya, Polynorbornene/MMT nanocomposites via surface-initiated ROMP: synthesis, characterization, and dielectric and thermal Properties, Journal of Materials Science, 49 (2014) 749-757.
16. E.E. Yalcinkaya, In situ synthesis of poly(N-vinylimidazole)/montmorillonite nanocomposites using intercalated monomer and thermal properties, Journal of Composite Materials, 50 (2016) 533-542.
17. F.Demir, B. Demir, E.E. Yalçınkaya, S.Çevik, D.O. Demirkol, Ü.Anık, S.Timur, Amino Acid Intercalated Montmorillonite: Electrochemical Biosensing Applications, RSC Advances, 4 (2014) 50107-50113.
18. M. Kotal, A.K. Bhowmick, Polymer nanocomposites from modified clays: Recent advances and challenges, Progress in Polymer Science, 51 (2015) 127–187.
19. S.S. Ray, M.Okamoto, Polymer/Layered Silicate Nanocomposites: A Review from Preparation to Processing, Progress in Polymer Science, 28 (2003) 1539-1641.
20. Y.F. Shih, L.S. Chen, R.J.Jeng, Preparation and properties of biodegradable PBS/multi-walled carbon nanotube nanocomposites, Polymer, 49 (2008) 4602–4611.
21. M.Tian, C.D.Qu, Y.X. Feng,. Structure and properties of fibrillar silicate/SBR composites by direct blend process, Journal of Material Science, 38 (2003) 4917–4924.
22. G.Chen, D.Shen, Z.Qi, Shear-induced ordered structure in polystyrene/clay nanocomposite, Journal of Material Research, 2 (2000) 351-356.
23. J. Fan, S. Liu, G. Chen, Z. Qi, SEM Study of a Polystyrene/Clay Nanocomposite, Journal of Applied Polymer Science, 83 (2002) 66–69.

24. M. Zanetti, G. Camino, P. Reichert, R. Mülhaupt, Thermal behaviour of poly(propylene) layered silicate nanocomposites, Macomolecular Rapid Communication. 22 (2001) 176–80.

25. S. Bocchini, A. Frache, G. Camino, M. Claes, Polyethylene thermal oxidative stabilization in carbon nanotubes based nanocomposites, European Polymer Journal, 43 (2007) 2942–3222.